Study of the modulation transfer function using speckle photography

A. M. HAMED, H. EL-GHANDOOR, S. Y. EL-ZAIAT

Physics Department, Faculty of Science, Ain-Shams University, Cairo, Egypt.

A quadratic model of a truncated parabolic-wave object is proposed to represent a periodic test object. This test object is experimentally constructed using a multi-exposure specklegram which forms a pattern nearly equivalent to the model described. The imaging irradiance distribution is calculated from the convolution product of the object irradiance and the impulse response of the incoherent imaging system. The theoretical results of the imaging irradiance and the corresponding contrast of the imaging systemm are graphically represented. The theoretical curve of the contrast or modulation transfer function (MTF) showed an agreement with the experimental one obtained from the interference patterns of the modulated speckle.

1. Introduction

It is known that the output of a linear-invariant system (LIS) is given by the convolution product of the input signal with the impulse response of the system. Knowing the impulse response of the imaging system, we can determine the output of the system for any input signal from the convolution product. The imaging performance in an incoherent imaging system [1] is characterized by the MTF. This MTF is computed from the autocorrelation function of a uniform circular aperture. Hence, the intensity impulse response is calculated from the Fourier transform operated upon the MTF. Contrarily, in a coherent imaging [2]−[5], the amplitude impulse response is computed by operating the Fourier transform upon the coherent transfer function. Several authors [6]−[11] have theoretically investigated the images of an incoherent triangular-wave pattern by a slit aperture in the presence of defocusing. They used uniform circular apertures for the illumination of the imaging system.

This paper gives an account of the calculation of the MTF for an incoherent imaging system provided with circular aperture. The corresponding imaging properties for a truncated parabolic wave object are obtained. The truncated parabolic wave function is selected as a model for the following reasons. Firstly, the resulting interference pattern obtained from multi-exposure specklegram [12] is nearly equal to the model described. Secondly, this model of the periodic test object is free from any discontinuities (Gibbs phenomenon) appearing in the rectangular wave function which results in the distortion of the object. A proper selection of the numerical aperture of the imaging lens and the ratio of exposure times of the specklegram [12] are considered as important variants to the model described.

In this paper, the intensity distribution of the image is calculated from the convolution integral of the quadratic test object and the impulse response of an incoherent imaging system. The calculated values of the contrast obtained from the imaging irradiance are graphically represented. Also, the contrast is derived from the autocorrelation function of a uniform circular aperture. The experimental values of contrast, measured from the images of the test object are fitted with the corresponding theoretical curves.

2. Theoretical analysis

The transmittance of spatial frequencies from an object to the image plane is investigated by applying Fourier techniques. A truncated parabolic wave object is assumed. This periodic wave function, $G(x)$ with period 2π, is defined as follows:

$$G(x) = (a+b) - \omega^2 x^2, \quad -\pi \leqslant \omega x \leqslant \pi \tag{1}$$

where a and b are two constants. The mean irradiance $\langle G \rangle$ is calculated as follows:

$$\langle G \rangle = \frac{\int G(x)\mathrm{d}x}{\int \mathrm{d}x},$$

$$\langle G \rangle = \frac{\int\limits_{0}^{\pi/\omega} [(a+b) - \omega^2 x^2]\mathrm{d}x}{\int\limits_{0}^{\pi/\omega} \mathrm{d}x} = [(a+b) - (\pi^2/3)].$$

The corresponding modulation is $\pi^2/3$, as shown in Fig. 1, where $\omega = 2\pi v = 2\pi/p$ is the angular frequency and p is the period. The maximum intensity that is obtained at $x = 0$ is $I_{max} = (a+b)$, while the minimum value of intensity obtained at $x = \pi/\omega$ is $I_{min} = a+b-\pi^2$.
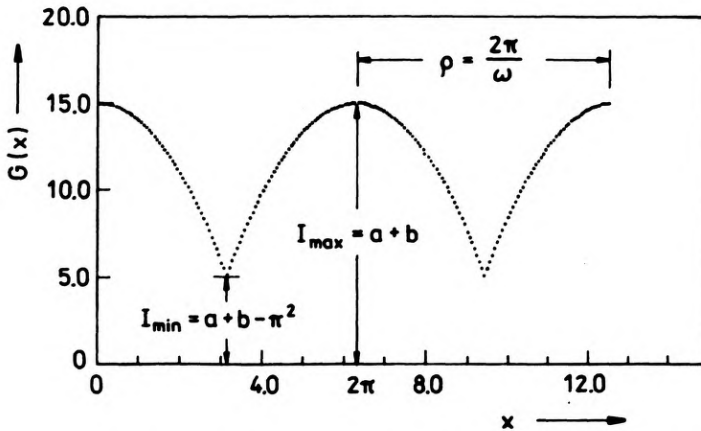

Fig. 1. Irradiance distribution of a truncated parabolic wave function of a test object, $a+b-\pi^2/3$ represents the mean irradiance and $\pi^2/3$ is the modulation

This periodic wave object is decomposed into sinusoidal components and these are imaged separately. The Fourier expansion [13] of the given function has the form

$$G(x) = (a+b) - \left[\frac{\pi^2 \omega^2}{3} + 4\omega^2 \sum_{n=1}^{\infty} \frac{(-1)^n}{n^2} \cos(n\omega x) \right].$$ (2)

The irradiance distribution in the imaging plane is calculated from the convolution product of the object irradiance and the impulse response of the incoherent imaging system [14]

$$I(x') = \int_{-\infty}^{+\infty} G(x) H(x' - x) \mathrm{d}x$$ (3)

or in a symbolic form

$$I(x') = G(x') * H(x')$$ (4)

where $H(x')$ is the image of an incoherent point object or the impulse response of the imaging system, and $*$ is a symbol for convolution. This impulse response of an incoherent system is calculated by taking the modulus square of the point spread function of a coherent system, *i.e.*

$$H(x') = |h(x')|^2$$ (5)

where: $h(x') = \text{FT}[p(u)]$ is the Fourier transform of the pupil function. It is known that the modulation transfer function is the autocorrelation function of the pupil aperture using incoherent imaging system, *i.e.*

$$\text{MTF} = \text{FT}[H(x')] = \text{FT}|h(x')|^2 = P(u) * P^*(u)$$ (6)

where $P(u) = \text{FT}[h(x')]$, and $*$ is a complex conjugate.

Since each harmonic component of the truncated parabolic-wave object is multiplied by the impulse response of the incoherent imaging system corresponding to that frequency, the irradiance distribution in the imaging plane is obtained as follows [11]:

$$I(x') = (a+b) - \sum_{n=1}^{n'} \left\{ \Gamma(n\omega) \left[\frac{\pi^2 \omega^2}{3} + \frac{(-1)^n}{n^2} 4\omega^2 \cos(n\omega x') \right] \right\}$$ (7)

where $\Gamma(n\omega)$ is a function which, for $n = 1$, reduces to the modulation transfer function of the imaging system. Because the system under consideration is aberration free, then we get the MTF by using Eq. (6) as follows [1]:

$$\Gamma(\omega') = \text{MTF} = \frac{2}{\pi} \left[\cos^{-1} \left(\frac{\omega'}{2} \right) - \frac{\omega'}{2} \left(1 - \frac{\omega'^2}{4} \right)^{1/2} \right]$$ (8)

where ω' represents the Fourier transform variable.

The impulse response of the incoherent imaging system may be approximately expressed by a triangular function of the form

$$H(x') = \Lambda(x') = 1 - |x'|, \quad |x'| \leqslant \lambda/\text{NA}.$$ (9)

Substituting from Eq. (9) and Eq. (2) in Eq. (3), the convolution integral becomes

$$I(x') = \int\limits_{-\infty}^{+\infty} \left[\left(a+b-\frac{\pi^2\omega^2}{3} \right) + 4\omega^2 \sum_{n=1}^{\infty} \frac{(-1)^2}{n^2} \cos n\omega x \right] H(x'-x)\mathrm{d}x. \tag{10}$$

This integral is decomposed into two separate integrals as follows:

$$I(x') = I_1 + I_2 \tag{11}$$

where the first integral is written as

$$I_1 = \int\limits_{x'-\lambda/\mathrm{NA}}^{x'+\lambda/\mathrm{NA}} \left[\left(a+b-\frac{\pi^2\omega^2}{3} \right)(1-x-|x'|)\mathrm{d}x \right] \tag{12}$$

and the second integral is

$$I_2 = \int\limits_{x'-\lambda/\mathrm{NA}}^{x'+\lambda/\mathrm{NA}} 4\omega^2 \sum_{n=1}^{\infty} \frac{(-1)^2}{n^2} \cos n\omega x(1-x-|x'|)\mathrm{d}x. \tag{13}$$

The first integral, Eq. (12), is analytically solved to obtain this result

$$I_1 = \left(a+b-\frac{\pi^2\omega^2}{3} \right)\left[\frac{2\lambda}{\mathrm{NA}} - \left(x'+\frac{\lambda}{\mathrm{NA}} \right)^2 \right]. \tag{14}$$

The second integral is also solved to obtain this result

$$I_2 = 8\omega^2 \sum_{n=1}^{N} \frac{(-1)^n}{n^2} \left\{ \frac{1}{n\omega}\left(\frac{\lambda}{\mathrm{NA}}+x' \right)\sin(n\omega x')\cos\left(\frac{n\omega\lambda}{\mathrm{NA}} \right) \right.$$
$$\left. + \left[\frac{(1+x')}{n\omega} \right]\cos(n\omega x')\sin\left(\frac{n\omega\lambda}{\mathrm{NA}} \right) - \frac{1}{n^2\omega^2}\sin(n\omega x')\sin\left(\frac{n\omega\lambda}{\mathrm{NA}} \right) \right\}. \tag{15}$$

Adding Eqs. (14) and (15), the imaging irradiance distribution becomes

$$I(x') = \left(a+b-\frac{\pi^2\omega^2}{3} \right)\left[\frac{2\lambda}{\mathrm{NA}} - \left(x'+\frac{\lambda}{\mathrm{NA}} \right)^2 \right] + 8\omega^2 \sum_{n=1}^{N} \frac{(-1)^n}{n^2}$$
$$\times \left\{ \frac{1}{n\omega}\left(\frac{\lambda}{\mathrm{NA}}+x' \right)\sin(n\omega x')\cos\left(\frac{n\omega\lambda}{\mathrm{NA}} \right) + \left[\frac{(1+x')}{n\omega} \right]\cos(n\omega x')\sin\left(\frac{n\omega\lambda}{\mathrm{NA}} \right) \right.$$
$$\left. - \frac{1}{n^2\omega^2}\sin(n\omega x')\sin\left(\frac{n\omega\lambda}{\mathrm{NA}} \right) \right\}. \tag{16}$$

The maximum intensity occurs at $\omega x' = 0$, thus using Eq. (16) we get

$$I_{max}(\omega x' = 0) = \left(a+b-\frac{\pi^2\omega^2}{3}\right)\left[\frac{2\lambda}{NA}-\left(\frac{\lambda}{NA}\right)^2\right]+8\omega^2\sum_{n=1}^{N}\frac{(-1)^n}{n^2}\left[\frac{1}{n\omega}\sin\left(\frac{n\omega\lambda}{NA}\right)\right].$$

(17)

The minimum intensity occurs at $\omega x' = \pi$, hence Eq. (16) becomes

$$I_{min}(\omega x' = \pi) = \left(a+b-\frac{\pi^2\omega^2}{3}\right)\left[\frac{2\lambda}{NA}-\left(\frac{\pi}{\omega}+\frac{\lambda}{NA}\right)^2\right]$$

$$+8\omega^2\sum_{n=1}^{N}\frac{(-1)^n}{n^2}\left[\frac{1}{n\omega}\left(1+\frac{\pi}{\omega}\right)\sin\left(\frac{n\omega\lambda}{NA}\right)\right].$$

(18)

The contrast of the fringes is obtained as

$$C = \frac{I_{max}-I_{min}}{I_{max}+I_{min}}.$$

(19)

Substituting from Eqs. (17) and (18) in Eq. (19), the contrast is computed as

$$C = \frac{\alpha A - 8\pi\sum_{n=1}^{N}\frac{(-1)^n}{n^2}\left(\frac{1}{n}\right)\sin\left(\frac{n\omega\lambda}{NA}\right)}{\alpha B + 8\pi\sum_{n=1}^{N}\frac{(-1)^n}{n^2}\left(\frac{2\omega}{n\pi}+\frac{1}{n}\right)\sin\left(\frac{n\omega\lambda}{NA}\right)}$$

(20)

where

$$\alpha = a+b-\frac{\pi^2\omega^2}{3}, \quad A = \frac{\pi^2}{\omega^2}+\frac{2\pi\lambda}{\omega NA} \quad \text{and} \quad B = \frac{2\lambda}{NA}\left(2-\frac{\lambda}{NA}\right)-\frac{\pi}{\omega}\left(\frac{\pi}{\omega}+\frac{2\lambda}{NA}\right).$$

3. Theoretical results

A computer program is constructed to calculate the imaging irradiance distribution of the quadratic test object, using Eq. (7), for two different spatial frequencies $\omega = 0.5$ and $\omega = 1$. The normalized irradiance distribution is shown in Fig. 2. It is shown that the image is sharper for greater values of ω. The convolution integral, Eq. (3), is analytically solved to obtain the imaging irradiance distribution. A triangular function is assumed to represent the impulse response of the imaging system. The imaging irradiance versus the spatial coordinate x' is computed for two different values of the spatial frequency by using Eq. (16). The calculated results are plotted as shown in Fig. 3. A program is made to compute the contrast versus the spatial frequency ω by using Eq. (20). These results are graphically represented as shown in Fig. 4 for two different values of NA = 0.4 and 0.6. It is shown that the contrast is sharply decreased in the range $0 \leqslant \omega \leqslant 0.9$ and then increased for higher values of $\omega > 0.9$ at NA = 0.6. The contrast is slowly decreased in the range $0 \leqslant \omega \leqslant 0.6$
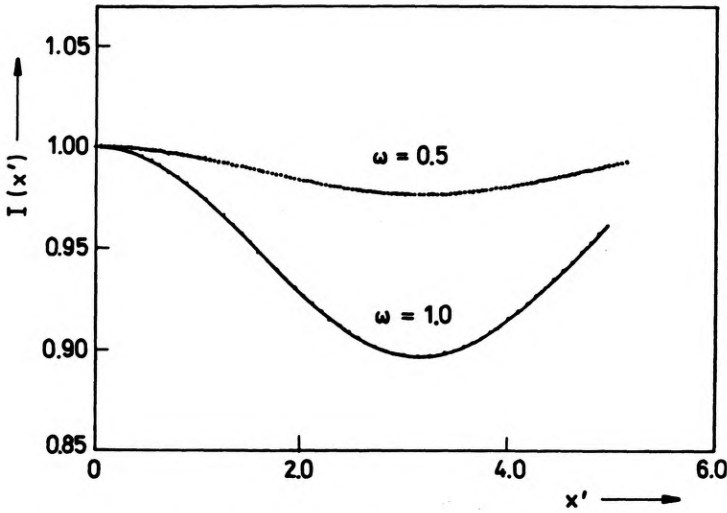
Fig. 2. Normalized irradiance distribution in the images for uniform aperture illumination of a truncated parabolic-wave object, where ω is the spatial frequency of the object
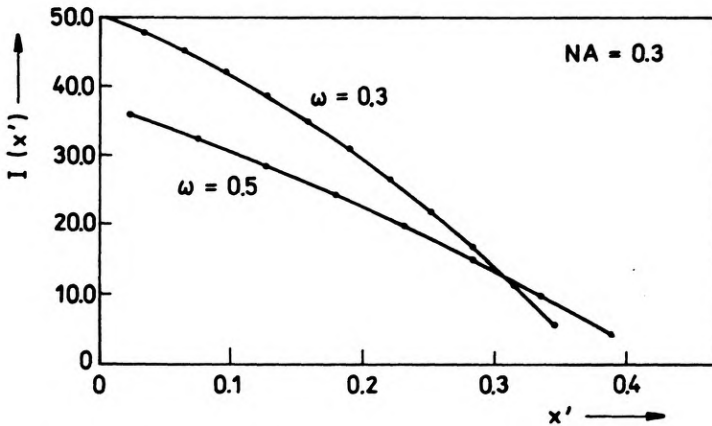

Fig. 3. Irradiance distribution in the images obtained using a truncated parabolic-wave object, where ω is the spatial frequency of the object

and then it is sharply increased for $\omega > 0.6$ at NA = 0.4. It should be noted that the contrast is improved for NA = 0.6 for higher values of spatial frequencies ω. Another curve of contrast versus NA at certain $\omega = 0.4$ is extracted from Eq. (20) as shown in Fig. 5.

4. Experimental results

The experimental set-up used in this work is shown in Figure 6a. It consists of a He-Ne laser source of wavelength $\lambda = 632.8$ nm which is used to illuminate
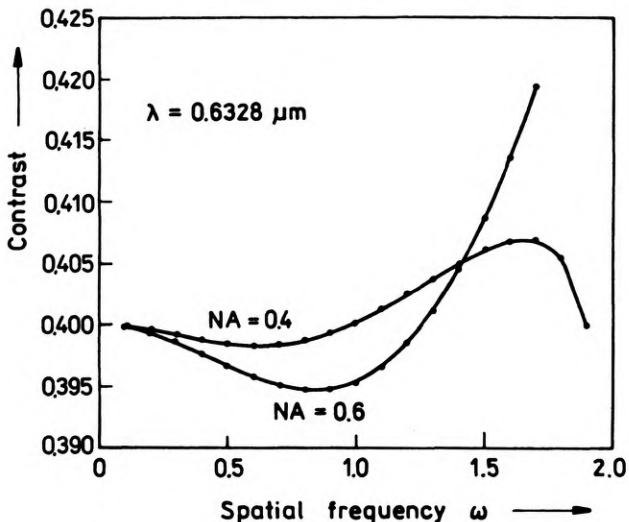
Fig. 4. Contrast C versus spatial frequency ω using a truncated parabolic-wave object
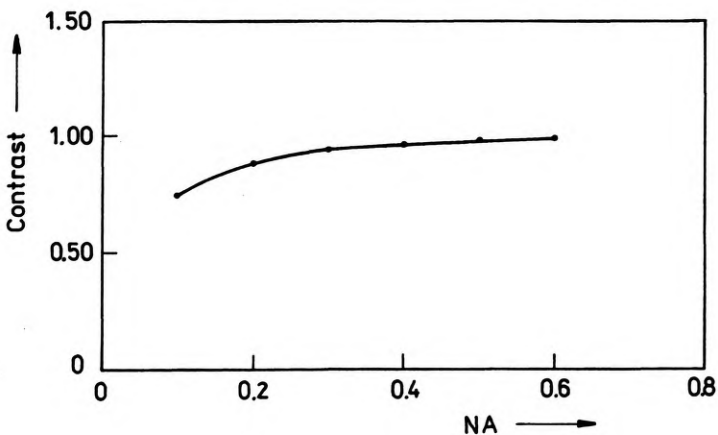
Fig. 5. Theoretical curve of contrast versus NA using a truncated parabolic object at $\omega = 0.4$
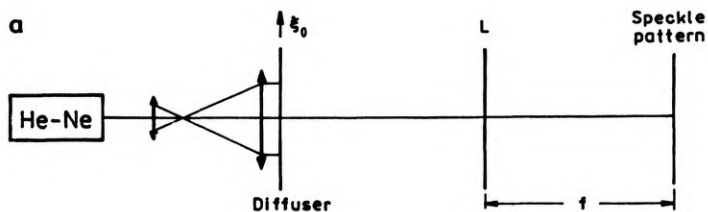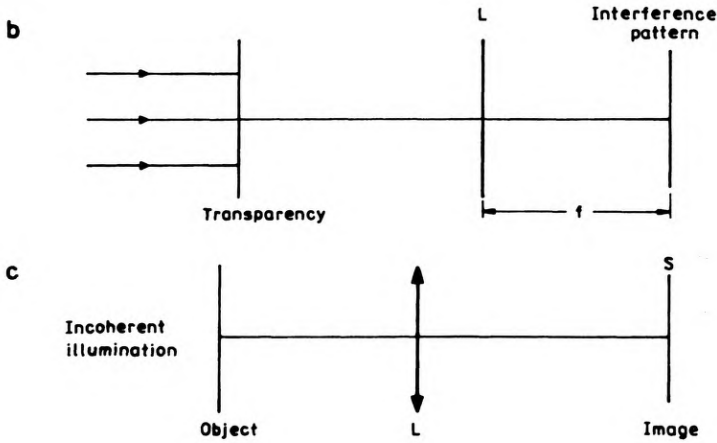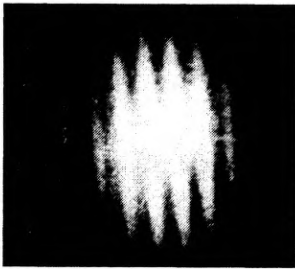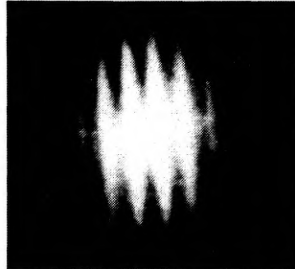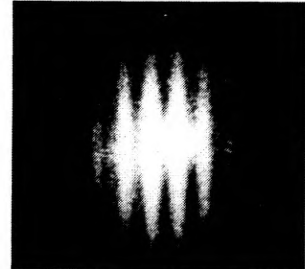

Fig. 6a

Fig. 6. Recording of multi-exposure specklegram, where $\xi_0 = 60$ μm is the displacement subjected to the diffuser (a), reconstruction process to visualize the interference pattern used as a test object (b), incoherent imaging using the interferogram as a test object, where L is the testing lens of focal length f (c)
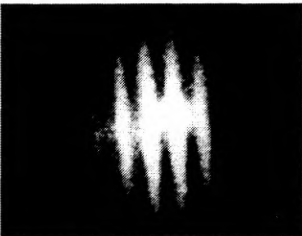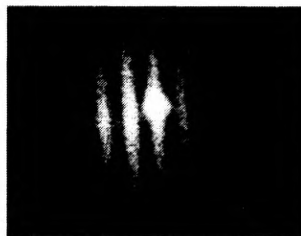

Fig. 7. Interferograms imaged by a testing lens using incoherent imaging of different numerical apertures

the specklegram forming the interference fringes on a screen *S* placed at a sufficiently great distance. This specklegram is obtained by taking three exposures on the same photographic plane. Equal displacements of 30 μm have been taken between exposures with the ratio of binomial coefficient 1:2:1 in order to obtain sharper fringes and to suppress the secondary fringes [12]. The obtained interference fringes are utilized as a test object as shown in Fig. 6b. Now, this test object is incoherently imaged using a lens of focal length $f = 5$ cm manufactured in the former USSR (Helios-44M-4) and of variable pupil aperture as in Fig. 6c.

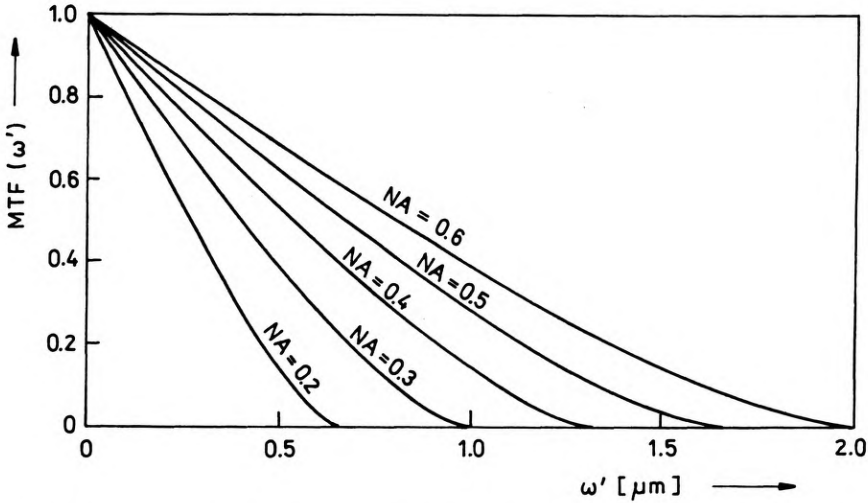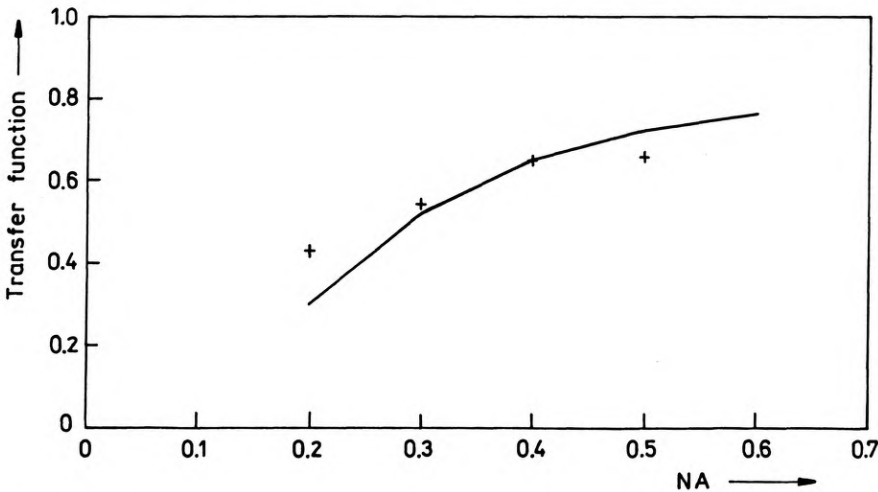Fig. 8. Modulation transfer function vs. spatial frequency for different NA = a/f at $\lambda = 0.6$ μm

Fig. 9. Transfer function vs. numerical aperture NA at a spatial frequency $\omega' = 0.4$ μm, where the cut-off spatial frequency $r_c = \lambda/\text{NA}$ (+ experimental values)

The incoherent imaging of the test object using apertures of NA = 0.1, 0.2, 0.3, 0.4 and 0.5 is shown in Fig. 7. The contrast obtained by measuring the visibility of the fringes is considered as a measure of the modulation transfer function [11]. A set of theoretical curves of MTF of an incoherent imaging system (Eq. (8)) are plotted in Fig. 8. The experimental values, extracted from Fig. 7, of the contrast obtained for different values of NA with the corresponding theoretical values at a spatial frequency $\omega' = 0.4$ are plotted in Fig. 9.

5. Conclusion

The formation of interference fringes using multi-exposure specklegam is utilized as a test object. The quadratic model of a truncated parabolic wave object is approved in this study. The MTF of an incoherent imaging system, using the interferogram as a test object, is obtained from the contrast curve for different NA of the imaging lens under test. The calculated contrast for the test object and that obtained from the autocorrelation function of the pupil aperture are in agreement with its experimental values.

References

[1] GOODMAN J. W., *Introduction to Fourier Optics*, McGraw-Hill Co., New York 1968.
[2] SHEPPARD C. J. R., WILSON T., Phil. Trans. Roy. Soc. A **295** (1978), 513.
[3] NOMARSKI G., J. Opt. Soc. Am. **65** (1975), 1166.
[4] CLAIR J. J., HAMED A. M., Optik **64** (1983), 133.
[5] HAMED A. M., CLAIR J. J., Optik **64** (1983), 277.
[6] LOHMANN A. W., Optik **14** (1957), 669.
[7] FORSTNER A., KOHLER H., Optik **17** (1960), 434.
[8] ROHLER R., Optik **19** (1962), 487.
[9] LOHMANN A. W., Appl. Opt. **5** (1966), 669.
[10] SINGH K., CHOPRA K. N., J. Opt. Soc. Am. **59** (1969), 1639.
[11] SINGH K., CHOPRA K. N., J. Opt. Soc. Am. **60** (1970), 641.
[12] BURCH J. M., TOKARSKI J. M. J., Opt. Acta **15** (1968), 101.
[13] PISKUNOV N., *Differential and Integral Calculus*, Mir Pub., Moscow 1969.
[14] BRACEWELL R. N., *The Fourier Transform and its Application*, McGraw-Hill Co., New York 1978.